Fuel 232 (2018) 845–854

Contents lists available at ScienceDirect

Fuel

journal homepage: www.elsevier.com/locate/fuel

Full Length Article

A proposed biomass char classification system

Edward Lester[a,*], Claudio Avila[a], Cheng Heng Pang[a,d], Orla Williams[a], Joseph Perkins[a], Sanyasi Gaddipatti[b], Gregory Tucker[b], Juan Manuel Barraza[c], María Patricia Trujillo-Uribe[c], Tao Wu[d]

[a] Faculty of Engineering, University of Nottingham, University Park, NG7 2RD Nottingham, United Kingdom
[b] School of Biosciences, Division of Nutritional Sciences, University of Nottingham, Sutton Bonington Campus, LE12 5RD Leicestershire, United Kingdom
[c] Facultad de Ingeniería, Universidad Del Valle, Ciudad Universitaria Meléndez, Calle 13 # 100-00. A. A., Cali, Colombia
[d] Division of Engineering, University of Nottingham, 315100 Ningbo, China

GRAPHICAL ABSTRACT

A sunflower particle showing how the internal structuring present in the original particle can influence the morphology of the char particles post pyrolysis.

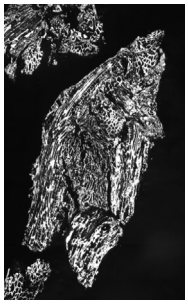

ARTICLE INFO

Keywords:
Biomass char
Morphology
Cellular
Porosity
Aspect ratio
Solids
Pyrolysis

ABSTRACT

A new classification system is proposed for the morphological characterisation of char structures from biomass. These char structures are unlike the coal chars that have an established nomenclature via the International Committee of Coal and Organic Petrology (ICCP) which divides char structures into thin walled and thick walled spheres and networks, mixed dense and mixed porous, fusinoids and solids. The chars from biomass show a tendency, depending on heating regime, to produce different types of internal pore structure (cellular and porous) and aspect ratio (high and low) compared with coal chars. For this reason a new classification system has been developed to cover these new structures which should assist in combustion, co-firing and gasification research where these intermediate char structures play an important role in conversion efficiency. Low heating rates (using a muffle furnace at 1000 °C and 3 min) were used to create chars from 9 different biomass types, with a range of lignocellulosic compositions. Char type appeared to depend on the biomass type itself and original lignocellulosic composition (cellulose, lignin and hemicellulose content) and cell structure.

1. Introduction

The use of biomass for energy production is increasing in many parts of the world, either through blending with fossil fuels or firing as a fuel in its own right. Biomass is considered to be CO_2-neutral [1–6] and therefore plays of a role in CO_2 reduction strategies. Biomass also has the additional benefit of inherently lower levels of sulphur [2,3,7] and nitrogen [2,7], in most cases. However, there are significant differences when compared to coal in terms of

* Corresponding author.
E-mail address: Edward.lester@nottingham.ac.uk (E. Lester).

https://doi.org/10.1016/j.fuel.2018.05.153
Received 20 March 2018; Received in revised form 23 May 2018; Accepted 29 May 2018

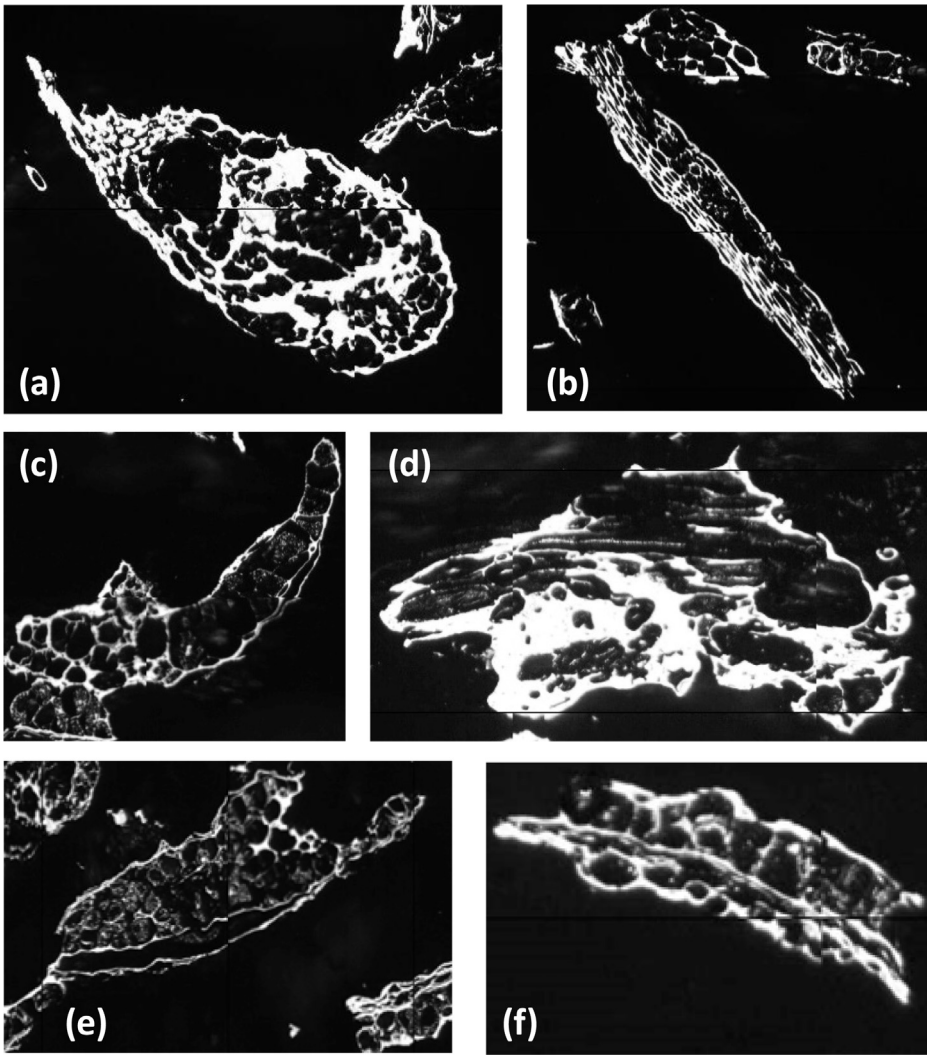

Fig. 1. Examples of low (a) and high (b) aspect ratio, thin wall (c) and thick wall (d), porous (e) and cellular (f) for wheat shorts chars.

higher moisture and volatile contents and lower levels of fixed carbon and ash [8]. However, despite these differences, they both follow comparable reaction stages during conversion [9,10]:

i. *Pyrolysis* – the devolatilisation and volatile release of materials, which often soften and swell while ejecting gaseous products of moisture and hydrocarbons, resulting in the formation of carbon-rich char
ii. *Conversion* of the intermediate carbon rich char particles in the presence of an oxidant gas, i.e. combustion
iii. *Deposition* or collection of mineral residues along with any unburnt carbon particles

Generally, a degree of overlapping occurs between step (i) and (ii) [11–13], however the process by which fuels are converted to heat are principally the same, as is the need to understand how these carbon structures from step (ii) affect the overall conversion efficiency. Much work has been focussed and published on coal char investigations [10,11,14–29], including the link between coal macerals and their associated char morphotypes [11,22,28]. The link between biomass characteristics and char morphology is less well known.

Biomass has three major lignocellulosic components, namely cellulose, hemicellulose and lignin. These three components are the major constituents of plant cell walls, a substantial portion of the dried biomass [30], and make up to over 90 wt% of the plant cells on an air-dry basis [31]. Cellulose is composed of long chains of cellobiose units [32], lignin is a complex, high-molecular-weight structure containing cross-linked polymers of phenolic monomers, and hemicellulose consists of branches of short lateral monosaccharides [33]. The glucose produced during photosynthesis is converted either into cellulose, which makes up the main structural component in cell walls, or stored in the form of starch granules in amyloplasts [33,34]. Starch is stored in tree twigs, fruits seeds, rhizomes, and tubers for the next growing season. The cellulose in cell walls are packed into microfibrils by the long-chain cellulose polymers linked by hydrogen and Van der Waals bonds, which are protected by hemicellulose and lignin [33]. The percentage of each component varies by biomass, and the influence of biomass composition on biomass char formation has not been explored in literature.

Recently, there has been an increase in the number of biomass char studies [35–38]. The morphology of the char structures has been analysed via Scanning Electron Microscopy (SEM) imaging [39–41] and optical microscopes [42,43]. With the increasing body of work into biomass chars, there is a need for a classification system to characterise the chars which accommodates the variances in structure compared to coal chars. Coal char has the following discriminating features [10];

1. *Char Wall-Thickness* – there has always been a distinction made between thin walled (classically known as *tenui*-) and thick walled (known as *crassi*-) chars. Differences in classification systems [44–47] are made around the threshold between thick and thin but most systems concede that chars generally can be seen as thick or thin – whereby the logic follows that thin chars will burn out more

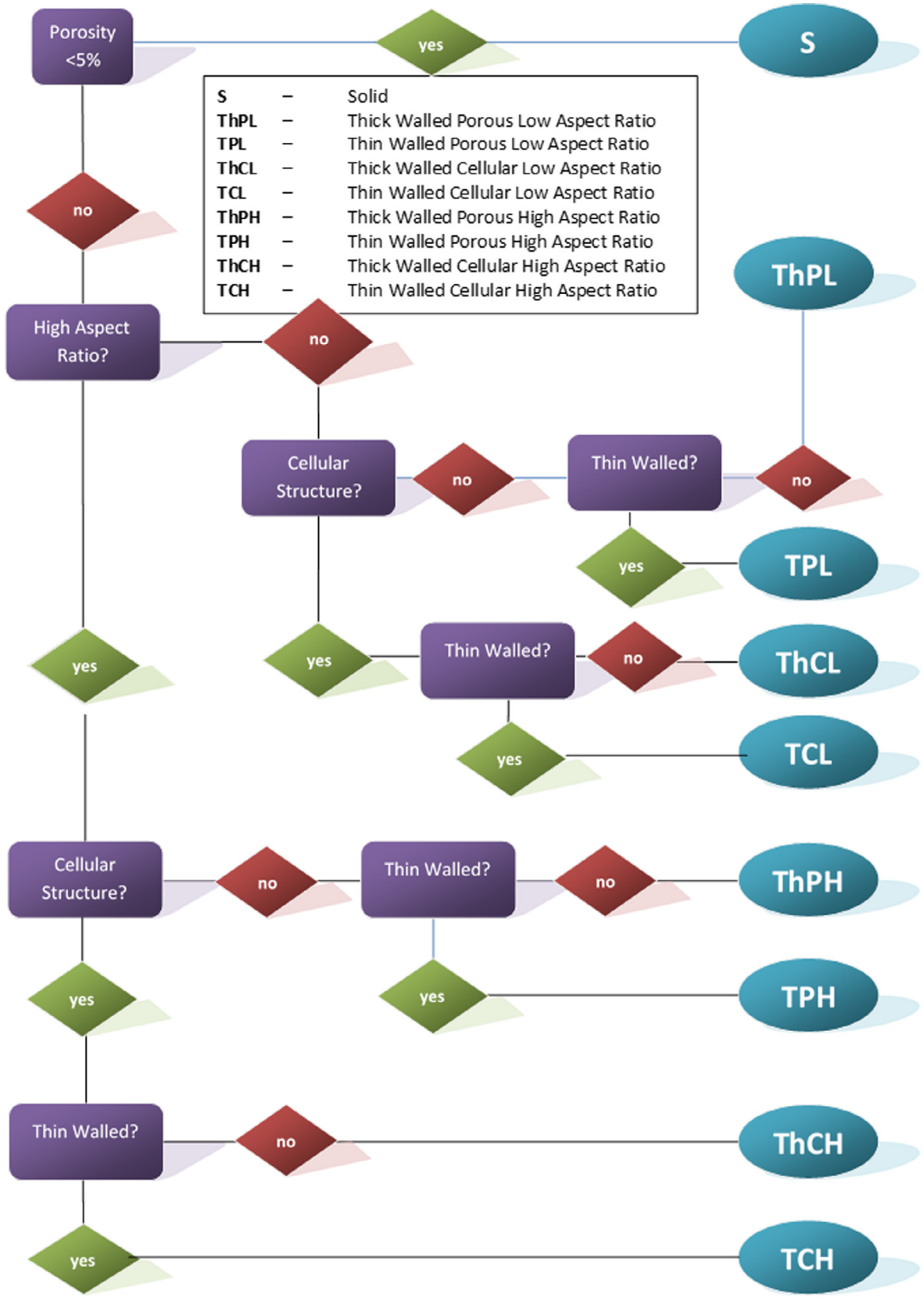

Fig. 2. Logic tree for classifying biomass chars types.

rapidly, and were derived from highly reactive material. Jenkinson [48] used wall thickness as one of the criteria in his char modelling system along with other characteristics such as NMR and ICP-MS data on mineral composition.

2. *Char Voidage and Porosity* – primary porosity includes larger central void (s), and secondary porosity which occurs as smaller voids located on char wall boundaries. The number and size of pores differentiates spherical particles (tenuisphere and crassisphere), from network particles

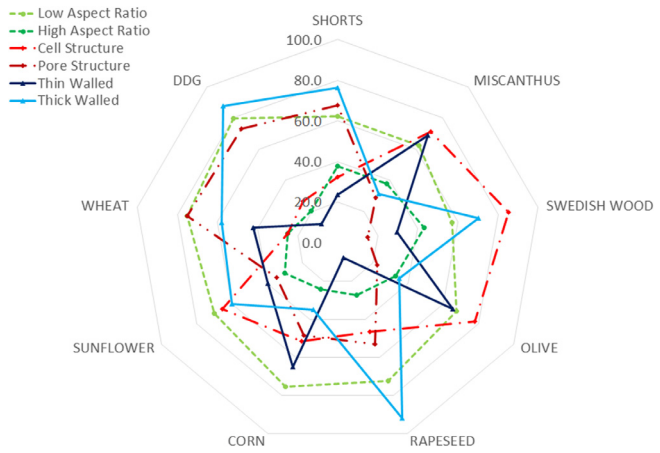

Fig. 3. Distribution of biomass char properties by biomass type.

(tenuinetwork, crassinetwork) and from mixed-porous and mixed-dense. Numerous pores of a reasonable size denote a network structure whereas up to 3 large open pores would define a sphere.

3. *Fused and unfused structures* – some coal macerals plasticise, vesiculate or swell and form new, potentially anisotropic structures [11,49]. The more reactive inertinite structures still structurally modify during heating [50]. 'Unreactive' components will tend to remain fused throughout the conversion process. Qian and co-workers discuss this in relation to biomass char, to some extent, but used SEM imaging of whole particles, rather than cross sections with oil immersion microscopy [51].

A biomass classification system needs to be as simple as possible whilst describing the main characteristics seen in biomass char. Ideally, the system needs to overlap with the current coal char classification system where necessary, not least to allow similarities between coal and biomass chars to be identified. The identified features should be of use for scientific study, whilst maintaining some relevance to end users e.g. working in utilisation related applications, such as combustion studies [52]. The proposed system draws on the characteristics (1) and (2) but discards the third, introducing aspect ratio as a more useful feature, not least because the aerodynamics of the particle will be dictated, in part, by its shape and density (which relates to (1) and (2)) [53]. The aerodynamics of the particulates in the flame, particularly as biomass particles can up to 3 mm in diameter, can make a large difference in determining whether the particle is entrained (leading to burnout), or falls out of the flame (to be collected in the furnace bottom ash [54]).

2. Experimental

2.1. Biomass samples

Nine different biomasses were analysed in this study; namely wheat and wheat shorts, miscanthus, olive residue, Swedish wood, corn stover, rapeseed, sunflower seed, and distillers dried grain (DDG). These 9 different types of biomass were dry sieved into different size fractions (namely 1180–600 µm, 600–300 µm, 300–212 µm, 212–106 µm, 106–75 µm, 53–75 µm).

2.2. Char preparation

To better understand how char morphology is affected by heating rate, the biomass char samples were prepared via slow heating using a laboratory muffle furnace. Ceramic crucibles were filled with 10 g of fresh biomass and a closed ceramic lid (to allow pyrolysis but with reduced air ingression in order to minimise combustion) and placed directly into a preheated fixed bed furnace at 1000 °C. Samples were left for 3 min, to allow the pyrolysis stage to be completed, after which the crucibles were removed and placed in a desiccator to avoid any ingress of moisture. This method has been described in more detail previously [9,10]. The muffle furnace treatment would be closer to a fluidised bed process or stoker system [55] rather than a pulverised fuel combustion flame [24].

2.3. Oil immersion microscopy

Scratch free, polished blocks were prepared using epoxy liquid resin for each sample in order to be characterized. A Zeiss Leitz Ortholux II POL-BK microscope with a 32x oil-immersion objective (and an internal 10x lens) providing a total of 320X magnification was used to analyse particle morphology. Composite images (3090 × 3900 pixels) from mosaics of 15 × 15, representing a total area of 4 mm × 3.3 mm, were obtained from the Zeiss AxioCam digital camera attached to the microscope and operated with KS400 V3.1 software.

2.4. Lignocellulosic composition analysis

The lignocellulosic compositions of all the raw biomass samples were determined using standard chemical assay tests with an estimated repeatability of ± 10% [56]. Lignin was determined via the standard acetyl bromide method [57]. 100 mg of biomass sample were added to a glass centrifuge fitted with a Teflon lined screw cap. 10 ml of acetyl bromide in acetic acid (250 ml) solution was added, capping immediately. The tube was heated in a water bath of 50 °C for 2 h with stirring at 30 min intervals. Upon cooling, the material was centrifuged at 2000 × *g* for 15 min. Around 0.5 ml of the solution was pipetted into a test tube containing 6.5 ml of glacial acetic acid and 2 ml of 0.3 M NaOH. After stirring, 1 ml of 0.5 hydroxylamine hydrochloride solution was added. All contents were stirred. Absorption spectra were determined for all samples. The absorption maxima at 280 nm were used to calculate lignin concentration using the equation proposed by Fukushima and Kerley [58]:

$$L = \frac{A - 0.0009}{23.077} \quad (1)$$

where L is the lignin concentration (mg/ml) and A is the absorbance.

The concentrations of hemicellulose and cellulose were determined using the potassium hydroxide (KOH) fractionation method [59] after the removal of the lignin (via the sodium chlorite method proposed by Ishizawa et al. [60]). The hemicellulose was isolated by extraction using 20 ml of 4 M KOH at room temperature for 2 h. A sample to liquor ratio of 1:20 was used. The resultant extract liquor was adjusted to pH 5 by the addition of 6 M acetic acid, followed by precipitation of the hemicellulose using acetone. The hemicellulose was washed with ethanol and water, followed by drying under vacuum at 60 °C. The final unextracted residue was weighed and classed as cellulose.

3. Classification system

The proposed biomass char classification system is based on three morphological characteristics: aspect ratio, wall thickness, and porosity. The key to any successful classification system is simplicity and the use of criteria that can be easily distinguished by a manual operator. The following sections evaluate the potential variances, and define the classification system for future users.

3.1. Aspect ratio

Some biomass chars can have significantly higher aspect ratio (ratio of length to width) than seen in coal chars, presumably because of their fibrous nature and their resistance to fracturing during milling [53] and the ability of the internal components to maintain their shape during devolatilisation [61]. It is acknowledged that the type of mill can probably influence aspect ratio i.e. ball milling will induce a different breakage mechanism compared to a ring roller mill [62]. By evaluating all images, (summarised in Fig. S1 in the Supplementary data) two classifications are proposed – *Low Aspect Ratio* and *High Aspect Ratio*. If the aspect ratio is 3 or higher, the particle should be classed as High Aspect Ratio.

Table 1
Biomass char property groupings by particle size (μm).

Acronym	Miscanthus (μm)						Swedish WOOD (μm)						Corn (μm)					
	1180–600	600–300	300–212	212–106	106–75	53–75	1180–600	600–300	300–212	212–106	106–75	53–75	1180–600	600–300	300–212	212–106	106–75	53–75
TCL	16.8	21.6	13.6	13.8	40.8	17.6	13.4	13.8	6.5	4.4	2.4	10.0	24.8	17.0	34.0	23.4	8.0	6.4
TCH	24.8	36.8	18.4	21.0	8.0	13.6	15.2	13.6	49.2	14.4	13.4	0.0	35.2	22.8	21.0	22.6	0.8	0.0
TPL	22.4	7.2	22.4	26.6	20.8	51.2	0.9	1.8	3.2	2.8	4.2	6.0	9.6	28.5	21.8	22.6	42.4	39.2
TPH	1.6	0.0	10.4	0.0	0.0	4.0	0.0	0.0	0.8	0.0	0.8	1.8	0.8	6.4	0.8	1.6	0.0	0.0
ThCL	11.2	23.2	12.8	20.2	19.2	6.4	33.8	27.2	16.0	24.3	44.2	67.2	14.4	9.8	4.0	11.2	13.6	9.6
ThCH	21.6	11.2	20.0	17.6	9.6	7.2	33.0	29.0	15.4	36.0	22.6	5.8	11.2	7.4	7.2	4.0	0.8	0.0
ThPL	1.6	0.0	2.4	0.8	1.6	0.0	0.9	12.0	8.2	17.0	12.4	9.2	4.0	8.2	11.2	10.6	33.6	44.8
ThPH	0.0	0.0	0.0	0.0	0.0	0.0	2.8	2.6	0.8	1.0	0.0	0.0	0.0	0.0	0.0	4.0	0.8	0.0
	Olive (μm)						Wheat (μm)						Wheat shorts (μm)					
	1180–600	600–300	300–212	212–106	106–75	53–75	1180–600	600–300	300–212	212–106	106–75	53–75	1180–600	600–300	300–212	212–106	106–75	53–75
TCL	24.0	25.6	20.8	28.4	29.2	44.4	2.4	6.0	6.8	1.8	2.4	0.0	1.2	1.6	2.4	4.0	0.0	0.0
TCH	40.8	21.6	22.4	10.8	11.8	2.4	28.0	15.0	11.1	5.6	0.0	0.0	31.0	24.8	20.0	3.0	0.0	0.0
TPL	0.0	0.8	11.2	23.8	25.0	44.2	26.4	18.4	34.2	15.6	13.6	6.4	4.4	9.8	10.4	8.6	4.2	0.0
TPH	0.0	0.0	0.8	1.6	1.6	0.0	20.8	24.4	10.3	3.8	0.0	0.0	5.6	5.4	3.2	2.8	0.0	0.0
ThCL	16.8	23.2	20.0	17.2	21.6	3.4	2.4	6.0	18.8	13.0	8.6	1.0	6.0	9.4	6.4	2.8	4.0	0.0
ThCH	17.6	28.8	16.8	13.2	4.2	0.8	6.4	9.2	2.6	3.4	0.0	0.0	34.0	18.0	16.0	9.8	0.0	0.0
ThPL	0.8	0.0	6.4	5.0	6.6	4.8	13.6	17.6	15.4	52.6	75.4	92.6	8.8	20.4	29.6	50.6	89.2	99.2
ThPH	0.0	0.0	1.6	0.0	0.0	0.0	0.0	3.4	0.9	4.2	0.0	0.0	8.8	10.6	12.0	18.4	2.6	0.8
	Rapeseed (μm)						DDG (μm)						Sunflower (μm)					
	1180–600	600–300	300–212	212–106	106–75	53–75	1180–600	600–300	300–212	212–106	106–75	53–75	1180–600	600–300	300–212	212–106	106–75	53–75
TCL	0.0	1.6	4.8	0.0	0.0	0.0	2.6	3.2	0.8	4.2	1.0	0.0	6.4	4.0	9.0	9.2	17.4	2.8
TCH	1.6	0.0	0.0	0.0	0.0	0.0	1.6	3.2	0.8	2.6	0.0	0.0	17.6	9.6	5.0	9.2	8.4	2.0
TPL	2.4	6.6	16.0	10.8	0.0	0.0	9.6	10.6	5.9	5.0	6.0	5.4	9.6	4.8	5.6	12.6	41.2	59.4
TPH	1.6	2.4	0.0	0.0	0.0	0.0	3.2	0.8	5.0	0.8	0.8	0.0	2.4	0.0	1.6	0.8	0.0	0.0
ThCL	25.6	13.0	10.4	21.4	40.2	9.0	9.6	13.0	15.0	10.0	6.8	3.2	16.8	37.6	43.0	43.7	13.8	15.0
ThCH	44.0	52.0	29.6	26.2	1.0	0.0	29.4	18.0	12.6	10.8	12.0	0.0	40.8	37.6	25.2	18.4	0.0	0.0
ThPL	22.4	22.0	39.2	41.0	57.8	91.0	41.6	49.6	55.6	61.6	67.4	89.4	4.0	6.4	10.6	6.0	19.2	20.8
ThPH	2.4	2.4	0.0	0.8	1.0	0.0	2.4	1.6	4.2	5.0	6.0	2.0	2.4	0.0	0.0	0.0	0.0	0.0

ThPL – Thick Walled Porous Low Aspect Ratio, **TPL** – Thin Walled Porous Low Aspect Ratio, **ThCL** – Thick Walled Cellular Low Aspect Ratio, **TCL** – Thin Walled Cellular Low Aspect Ratio, **ThPH** – Thick Walled Porous High Aspect Ratio, **TPH** – Thin Walled Porous High Aspect Ratio, **ThCH** – Thick Walled Cellular High Aspect Ratio, **TCH** – Thin Walled Cellular High Aspect Ratio.

The likelihood that a particle will form high aspect ratio chars rather than low aspect ratio is linked to particle size, heating rate and cellular structure [63,64]. If the cellular structure is quite developed, the high aspect particle will be able to swell during softening (assuming a high enough heating rate) and form a significantly wider particle, as illustrated in Fig. 1a for wheat shorts. This distinction should prove to be useful in combustion research where it has been shown that higher aspect ratio particles (described as cylindrical) burn faster than low aspect ratio particles (described as spherical) [65]. Particles of different shape will travel differently in the boiler. Flatter 'platelet-like' structures are more likely to be retained in the flame than denser, rounded particles. The latter would be more prone to fall through the boiler quickly if they have a low aspect ratio and mass [66].

3.2. Wall thickness

As with coal char, there are different ways to consider wall thickness, but in literature, 3–5 μm tends to be the threshold that defines the transition from thin walled chars to thick wall chars [10,67]. During manual analysis, the char particle that is identified by the cross hair must be assessed for wall thickness. Without the use of image analysis to measure the wall thickness of the whole char [68], the manual analyst must give a qualitative assessment of the 'general' thickness of the char. Regardless of the differences in burnout kinetics (there is a difference in burnout rates when comparing coal and biomass char [69], biomass to biomass [9], and a biomass to its torrefied form [70]) wall thickness is still a critical parameter since thick walled chars burn out more slowly than thin walled chars because of the diffusion limited reactions that take place in a boiler [71]. The proposed system distinguishes between thin walled biomass chars (that have a wall thickness of < 3 μm) and thick walled (that have a wall thickness > 3 μm) where the judgement around 'thickness' is based on the overall assessment of the whole char. Fig. 1 shows thin (Fig. 1c) and thick (Fig. 1d) walled chars for wheat shorts. Additional examples can be found in Fig. S2 in the Supplementary section.

3.3. Porosity

Two different types of pore were seen with all biomass types in this study; those that had clearly retained cellular porosity (based on typical initial cell walls seen in biomass) [72] and those where the porosity was more like open rounded pores seen in tenuisphere and crassisphere coal chars. Fig. 1e and Fig. 1f show examples of both these classes. Cellular char structures indicates controlled devolatilisation where the lignocellulosic structure remained intact allowing the controlled loss of volatiles through predefined channels and pores, while porous structures dictates structural softness and fluidity that indicates that the volatile release phase was less controllable. Coal chars are formed from the partial melting and fluidisation of the fixed carbon material during devolatilisation. Porous structures are those that show softening and/or enhance volatile/moisture release. Macro pores are larger and more consistent with coal char pores, as seen in tenuispheres and crassispheres. Some char particles can be clearly a mixture of both porous and cellular types. Cellular pore structures are similar to those seen in the original biomass cell structures where each cell appears more uniform and rounded, located next to many other similar sized cells. These cells bear most resemblance to inertinite structures in coal such as fusinite and semifusinite (which are formed from the oxidised cellulosic structures of plants, either through forest fires or slow autochthonous oxidation and ageing [73]). When defining cellular pores however, there is an issue with structural anisotropy or orientation of the particle in relation to the surface. In some cases, such as DDG and olive residue, cellular pores may appear to be more elongated. These internal structures are more like inertinite-derived char structures and result from sectioning along the length of the pores rather than at right angles. As with the cellular structures, there is no sign of extensive softening or swelling.

4. Application of the classification system to biomass chars

On the basis that there are 3 specific criteria to identify chars, i.e. aspect ratio, wall thickness and porosity, 9 groupings exist as follows. The chars were found to be either one of walled-porous-low aspect ratio (ThPL), thin walled-porous-low aspect ratio (TPL), thick walled-cellular-low aspect ratio (ThCL), thin walled-cellular-low aspect ratio (TCL), thick walled-porous-high aspect ratio (ThPH), thin walled-porous-high aspect ratio (TPH), thick walled-cellular-high aspect ratio (ThCH), thin walled-cellular-high aspect ratio (TCH), or solid (S). The solid category was added to describe all materials without any significant porosity ($< 5\%$) where wall thickness, in most cases, are thick walled. Whilst this category could be expanded to high and low aspect ratio solids, neither was seen in biomass chars i.e. no char was found to be completely solid with very low porosity. Even in coal, the creation of solids would normally only originate from sclerotinite or macrinite [74] (inertinite sub-macerals) or from heat affected coal or pet coke materials. Fig. 2 shows a logic tree that defines the decision making process required to identify each char type.

4.1. Influence of biomass type and particle size on char properties

Fig. 3 presents the overall char properties of the tested biomasses. Groupings can be made of chars with similar features, e.g. high aspect ratio particles (regardless of thick or thin, cellular or porous). Overall, the chars for all biomasses are predominately of low aspect ratio, indicating that swelling has probably occurred during combustion. DDG showed the highest proportion of low aspect ratio particles (80%) and Swedish wood the lowest (57%).

There was greater variance in the wall thickness of the chars, with DDG, Swedish wood, wheat shorts and rapeseed exhibiting predominately thick walled structures ($> 60\%$), while miscanthus, wheat, corn stover, olive and sunflower had a greater proportion of thin walled chars overall. Interestingly, wheat shorts and wheat showed opposite wall thickness trends, indicating that they have different pyrolysis kinetics despite being from the same plant.

Distinct trends can be seen for porosity, as miscanthus, Swedish wood, olive and sunflower chars are mainly composed of cell structures, while DDG, wheat shorts, wheat, and rapeseed have mainly porous char structures. Only corn stover showed a more balanced porosity with almost equal part cell (52%) and porous (48%) char structures.

The initial size of the biomass particles was found to impact the properties of the resultant chars (Table 1). Wheat shorts are predominantly TCH and ThCH at large particle sizes, but almost entirely ThPL for fines, indicating a fundamental change in structure and aspect ratio with decreasing particle size. Similar changes are also noted for DDG, wheat, and rapeseed. Swedish wood exhibited chars with increasing levels of cell-type structures, while olive showed more thin walled structures with decreasing particle size. Fig. 4 provides an indicative illustration of the trends in groupings as influenced by particle size, based on the data in Table S1 in the Supplementary data. Fig. 4a shows that for all the biomass chars, a larger initial particle size will result in a high aspect ratio for the resultant char. As particle size decreases, the aspect ratio reduces, suggesting that smaller particles either start with more spherical particles or that swelling is greater during combustion. Whilst coal particles can melt or soften and form spherical droplets, biomass char particles can be very irregular and shape is determined by the combined influence of the lignin structure of the original biomass and the mechanical process by which the particles are formed [64]. Pulverised wood can have either a spherical or cylindrical structure, but straw can have a cylindrical structure and the aspect ratio is determined by the degree of milling [53,64]. The majority of the samples show similar trends, but wheat shorts and sunflower particles exhibit a greater spread of char aspect ratios across their initial particle size distribution.

Three distinct trends were observed for the biomass char wall thickness and particle size (Fig. 4b). Wheat shorts, Swedish wood, olive and DDG char wall thickness increases with decreasing particle size, suggesting that the fines of these biomasses could take longer to burn out than larger particles with thinner walls [68]. Wheat and corn stover show the same trend, but with a greater proportion of thin walled chars at large particle sizes. Miscanthus, sunflower and rapeseed show the opposite trend to the other samples, with decreasing particle size

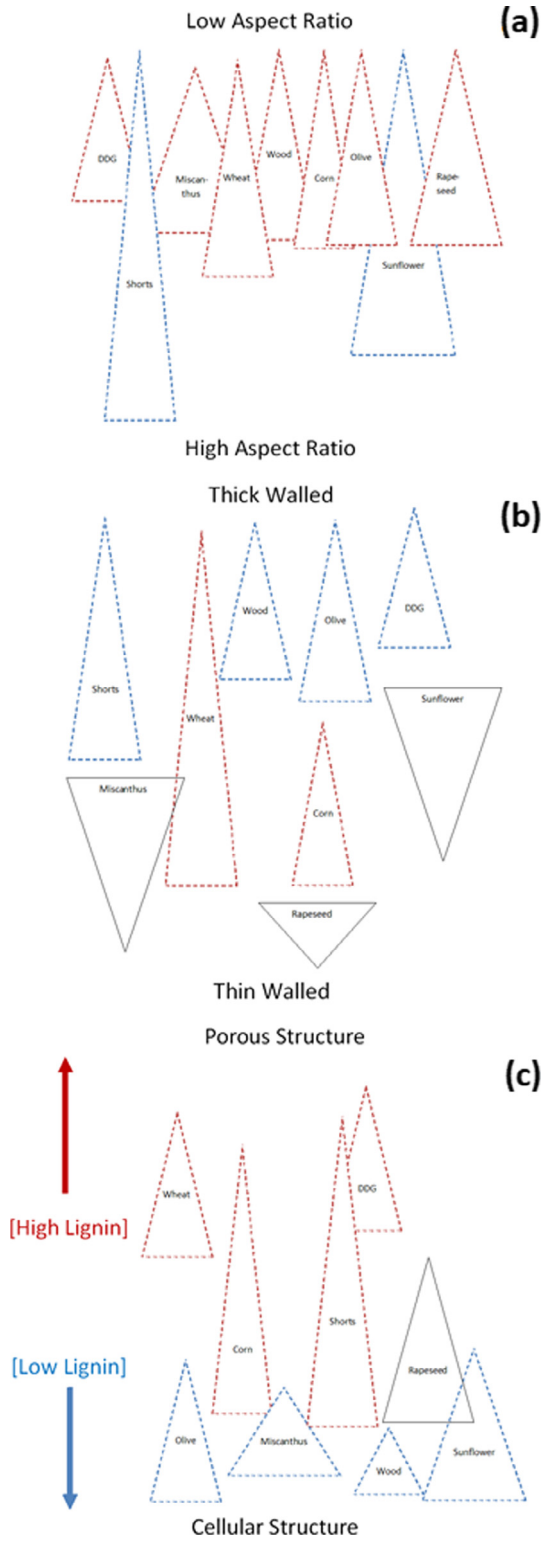

Fig. 4. Visualisation of influence of particle size on char aspect ratio for different biomass types (a), influence of particle size on char wall size for different biomass types (b), and influence of particle size on char porosity for different biomass types. The shape of the biomass triangle gives an indication of the changes with decreasing particle size range, with the wider edge being the largest particle size, and point the fines.

resulting in thinner char walls. Sunflower and rapeseed are both flowering plants and miscanthus is a grass species, while DDG, corn and wheat are cereal grain crops, olives are fruits. This variation in species may account for the distinct difference in char wall thickness.

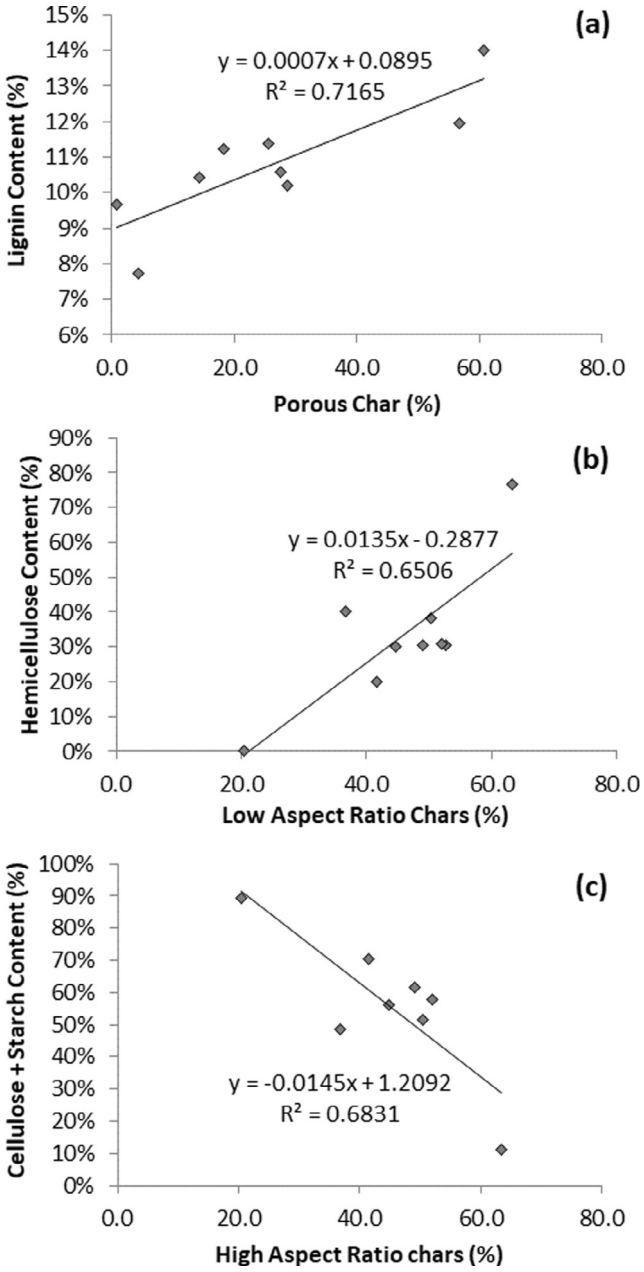

Fig. 5. Correlation between lignin content and porous chars (a), hemicellulose content and low aspect ratio chars (b), cellulose and starch content and high aspect ratio chars (c) for all biomasses.

For porosity (Fig. 4c), all biomass chars showed more cell structures for larger particles sizes, and more porous structures for fines. Olive, miscanthus, wood, and sunflower chars had predominantly cell structures across their particle size distribution, while wheat and DDG were mainly porous. Corn, wheat shorts and rapeseed showed a mix of cell and porous structures.

4.2. Influence of composition

It has been shown in several studies that coal macerals impact the associated char morphotype [11,22,28]. This study found that this was also true for biomass composition and the resultant char morphologies. Table 2 provides the composition of all the biomasses. Some biomasses contained mainly cellulose (olive), starch (wheat shorts) or hemicellulose (DDG), but all samples had lignin contents between 8 and 14%. Only corn, DDG, wheat shorts, and Swedish wood contained

Table 2
Biomass compositional components.

	Cellulose (%)	Lignin (%)	Starch (%)	Hemi-cellulose (%)	Starch and Cellulose (%)	Hemicellulose and Cellulose (%)
Corn	**24**	**10**	**36**	**30**	59	54
DDG	**1**	12	**10**	77	11	78
Miscanthus	**58**	11	**0**	31	58	89
Olive	**70**	10	**0**	20	71	90
Rapeseed	**51**	10	**1**	38	51	90
Wheat Shorts	**22**	11	**67**	0	89	22
Sunflower	**48**	11	**1**	40	48	89
Swedish Wood	**10**	8	**51**	31	62	40
Wheat	**56**	14	**0**	30	56	86

starch. By correlating the biomass composition to the resultant char properties, 3 strong trends were observed. The strongest correlation existed between lignin content and porous cells structures (Fig. 5a). This indicates that the higher the lignin content, the more likely the char will have open pores rather than a cellular structure. Increasing hemicellulose content results in lower aspect ratio chars (Fig. 5b) and increasing cellulose and starch content results in a decrease in the proportion of higher aspect ratio chars (Fig. 5c).

4.3. Structural components and char structure

All biomasses are composed of three different tissues: ground (parenchyma, sclerenchyma and collenchyma cells), vascular (xylem and phloem cells) and dermal tissues [75]. Each type of cell has its own unique characteristics, and thus it is possible to identify cells even when the biomass particles were milled into smaller fragments (Fig. 6). These characteristics include the number of cell wall layers, location, and lignocellulosic composition. In order to verify the identifications, a piece of un-milled raw miscanthus was examined across its cross section (Fig. 6a). For the un-milled raw miscanthus piece, some of the original plant cells have thicker cell walls, particularly for xylem and sclerenchyma cells. These cells are specialised in certain functions which require them to have both primary and secondary walls for an enhanced strength. Xylem cells require secondary thickening to withstand the negative pressure while conducting water, whilst sclerenchyma provides mechanical support to plants. Other less specialised cells with only primary walls, like parenchyma, appear to have thinner walls.

As mentioned in Section 3.1, the heating rate used in this paper

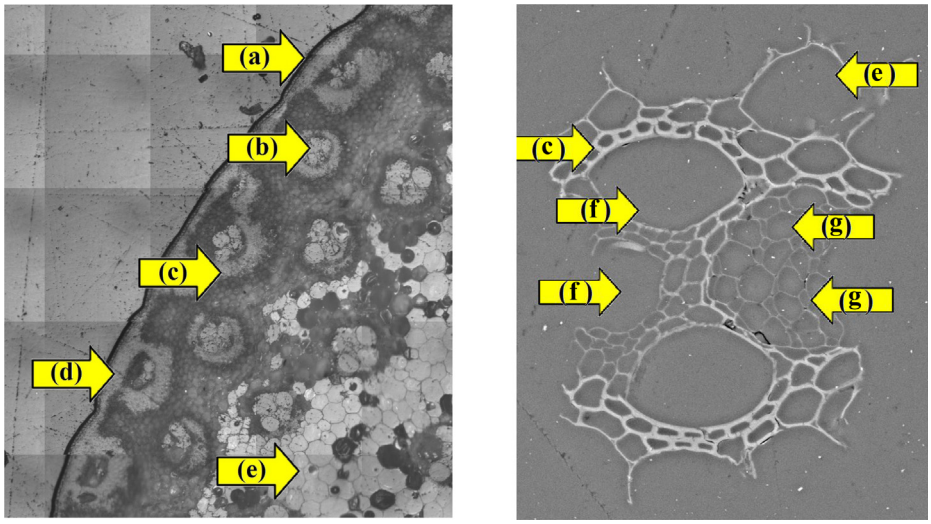

Fig. 6. Air optical microscope mosaic image of cross section of unmilled miscanthus piece (left) and SEM image of cross section of milled particle of miscanthus 212–300 μm (right). Identified components: (a) Epidermis; (b) Vascular bundle; (c) Bundle sheath, sclerenchyma cell; (d) Collenchyma cells (e) Parenchyma cell, (f) xylem cells; (g) phloem cells; Xylem and phloem are collectively known as vascular bundle.

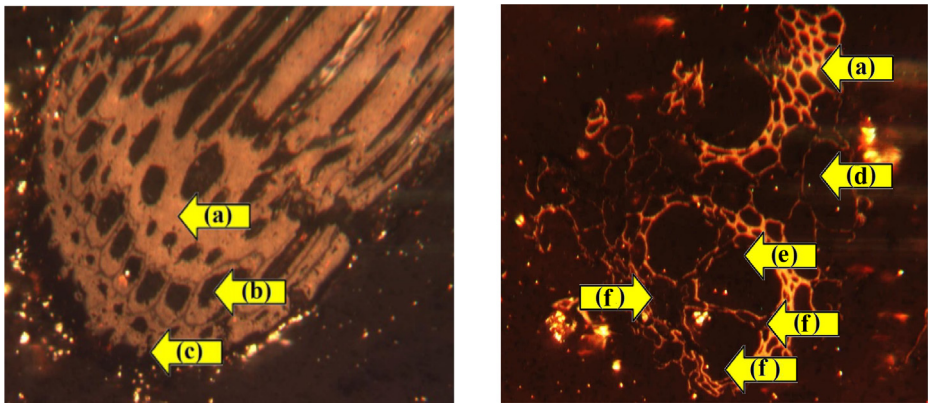

Fig. 7. Oil-immersion microscope image: Cross section of milled miscanthus char 212–300 μm. Identified components: (a) Sclerenchyma cell, bundle sheath, (b) Collenchyma cell, (c) Epidermis cell, (d) Parenchyma cell; (e) Phloem cell, (f) xylem cells.

allows the char particles to retain original biomass cell structures since the volatiles released during devolatilization stage have sufficient time to escape through existing cracks and natural pores [76]. This allows further identification of cells even after devolatilization (Fig. 7). Similarly, cells with both primary and secondary walls appear to have much thicker char walls compared to those with only primary walls. This is because secondary walls are inherently thicker and stronger, whilst its constituents are less accessible since the microfibrils are more orderly arranged [32].

The fact that secondary walls in biomass would produce chars with thicker walls makes the study of its constituents important. Normally, secondary walls have twice the cellulose content of primary walls [77]. Also, secondary walls are characteristically thickened with lignin, which is rarely found in primary walls [32]. The rigid lignin provides the necessary compressive strength and bending stiffness [32], while cellulose, through the winding of microfibrils, provides the required tensile strength, about twice that of a basic steel [78]. Thus, with adequate compressive and tensile strengths to prevent the tearing and expansion of cells (and compression of adjacent cells), coupled with the relatively low reactivity of cellulose and lignin, the original structure of biomass is retained during the rapid volatile and moisture release upon fast heating. However, the lack of such strengthening factors in 'weaker' cells with only primary walls makes the cell walls relatively easier to swell and rupture due to the internal pressure from volatile release, thereby breaking the boundaries between adjoining cells to produce thinner chars with larger pores.

Third generation biofuel residues such as micro and macro algae sources, and refuse derived fuels, may well create new char morphologies that not described by the classification system in this paper. Most of these biomass sources have cell-like structures (although RDF can be more than cardboard and paper and can even contain plastics) but more work is needed to confirm whether they behave differently during heating.

5. Conclusions

This paper presents a new classification system for the morphological characterisation of char structures from biomass. These char structures are unlike the chars seen from coals, and have a tendency to produce different types of internal pore structure and aspect ratios compared with coal chars. For this reason, a new classification system has been developed which classifies biomass chars by 3 parameters; aspect ratio, wall thickness and porosity. From this, 9 groups were found based on combinations of these parameters. Biomass chars were found to have predominantly low aspect ratios, which indicates swelling during combustion. Particle size also impact on the char porosity of individual biomasses, with larger particles producing higher aspect ratio chars in all cases.

Biomass composition was found to influence the resultant chars formed. Chars with high lignin and small particle sizes exhibited porous structures, large biomass particles with low levels of lignin tended to produce cellular structures.

The proposed biomass char classification system has the potential for adaption for new fuels and is the basis for a new image analysis technique currently under development. This classification system will assist in combustion. co-firing and gasification research where these intermediate char structures play an important role in conversion efficiency.

Acknowledgements

This work was supported by the Engineering and Physical Sciences Research Council [grant number EP/F060882/1, L016362/1], the last grant was provided by EPSRC Centre for Doctoral Training in Carbon Capture and Storage and Cleaner Fossil Energy, and the British Council Newton Fund Institutional Links [grant number 216427039] and the Natural Science Foundation China (NSFC) [Grant Number 51650110508]. Samples for the project were generously provided by Dr David Waldron at Alstom. The authors would like to thank all those involved in the project for their support and assistance.

Appendix A. Supplementary data

Supplementary data associated with this article can be found, in the online version, at http://dx.doi.org/10.1016/j.fuel.2018.05.153.

References

[1] Demirbas A. Sustainable cofiring of biomass with coal. Energy Conserv Manage 2003;44:1465–79.
[2] Sami M, Annamalai K, Wooldridge M. Co-firing of coal and biomass fuel blends. Prog Energy Combust Sci 2001;27:171–214.
[3] Demirbas A. Biomass resource facilities and biomass conversion processing for fuels and chemicals. Energy Convers Manage 2001;42:1357–78.
[4] Müller-Hagedorn M, Bockhorn H, Krebs L, Müller U. A comparative kinetic study on the pyrolysis of three different wood species. J Anal Appl Pyrolysis 2003;68–69:231–49.
[5] Gupta RB, Demirbas A. GDE gasoline, diesel and ethanol biofuels from grasses and plants. Cambridge University Press; 2010.
[6] Abbasi T, Abbasi SA. RES Renewable Energy Sources: Their Impact On Global Warming and Pollution. PHI Learning; 2010.
[7] Molcan P, Lu G, Le Bris T, Yan Y, Taupin B, Caillat S. Characterisation of biomass and coal co-firing on a 3 MWth Combustion Test Facility using flame imaging and gas/ash sampling techniques. Fuel 2009;88:2328–34.
[8] Vassilev SV, Vassileva CG, Vassilev VS. Advantages and disadvantages of composition and properties of biomass in comparison with coal: an overview. Fuel 2015;158:330–50.
[9] Avila C, Pang CH, Wu T, Lester E. Morphology and reactivity characteristics of char biomass particles. Bioresour Technol 2011;102:5237–43.
[10] Lester E, Alvarez D, Borrego AG, Valentim B, Flores D, Clift DA, et al. The procedure used to develop a coal char classification-Commission III Combustion Working Group of the International Committee for Coal and Organic Petrology. Int J Coal Geol 2010;81:333–42.
[11] Alonso MJG, Borrego AG, Álvarez D, Menéndez R. Reactivity study of chars obtained at different temperatures in relation to their petrographic characteristics. Fuel Process Technol 2001;69:257–72.
[12] Cetin E, Moghtaderi B, Gupta R, Wall TF. Influence of pyrolysis conditions on the structure and gasification reactivity of biomass chars. Fuel 2004;83:2139–50.
[13] Backreedy RI, Jones JM, Pourkashanian M, Williams A. Burn-out of pulverised coal and biomass chars. Fuel 2003;82:2097–105.
[14] Lu L, Kong C, Sahajwalla V, Harris D. Char structural ordering during pyrolysis and combustion and its influence on char reactivity. Fuel 2002;81:1215–25.
[15] Kelebopile L, Sun R, Liao J. Fly ash and coal char reactivity from Thermo-gravimetric (TGA) experiments. Fuel Process Technol 2011;92:1178–86.
[16] Zhang S, Hayashi JI, Li CZ. Volatilisation and catalytic effects of alkali and alkaline earth metallic species during the pyrolysis and gasification of Victorian brown coal. Part IX. Effects of volatile-char interactions on char-H2O and char-O2 reactivities. Fuel 2011;90:1655–61.
[17] Zhang H, Pu WX, Ha S, Li Y, Sun M. The influence of included minerals on the intrinsic reactivity of chars prepared at 900 C in a drop tube furnace and a muffle furnace. Fuel 2009;88:2303–10.
[18] Russell NV, Gibbins JR, Williamson J. Structural ordering in high temperature coal chars and the effect on reactivity. Fuel 1999;78:803–7.
[19] Olivella MA, De Las Heras FXC. Study of the reactivities of chars from sulfur rich Spanish coals. Thermochim Acta 2002;385:171–5.
[20] Gilfillan A, Lester E, Cloke M, Snape C. Structure and reactivity of density separated coal fractions. Fuel 1999;78:1639–44.
[21] Li Q, Wang Z, He Y, Sun Q, Zhang Y, Kumar S, et al. Pyrolysis characteristics and evolution of char structure during pulverized coal pyrolysis in drop tube furnace: influence of temperature. Energy Fuels 2017;31:4799–807.
[22] Lester E, Cloke M. Characterisation of coals and their respective chars formed at 1300 C in a drop tube furnace. Fuel 1999;78:1645–58.
[23] Cloke M, Lester E, Leney M. Effect of volatile retention on the products from low temperature pyrolysis in a fixed bed batch reactor. Fuel 1999;78:1719–28.
[24] Cloke M, Lester E, Belghazi A. Characterisation of the properties of size fractions from ten world coals and their chars produced in a drop-tube furnace. Fuel 2002;81:699–708.
[25] Cloke M, Lester E, Thompson AW. Combustion characteristics of coals using a drop-tube furnace. Fuel 2002;81:727–35.
[26] Chan M-L, Jones JM, Pourkashanian M, Williams A. The oxidative reactivity of coal chars in relation to their structure. Fuel 1999;78–13:1539–52.
[27] Feng B, Bhatia SK, Barry JC. Structural ordering of coal char during heat treatment and its impact on reactivity. Carbon N Y 2002;40:481–96.
[28] Alonso MJG, Borrego AG, Alvarez D, Parra JB, Menéndez R. Influence of pyrolysis temperature on char optical texture and reactivity. J Anal Appl Pyrolysis 2001;58–59:887–909.
[29] Sheng C. Char structure characterised by Raman spectroscopy and its correlations with combustion reactivity. Fuel 2007;86:2316–24.
[30] Dalimova GN, Burkhanova ND, Nikonovich GV. Separation of the lignocellulose of nonwoody plants into its main components and study of their properties. Chem Nat Compd 1998;34:92–5.
[31] Glazer AN, Nikaido H. Microbial biotechnology: fundamentals of applied

microbiology. Cambridge University Press; 2007.
[32] Evert RF. Esau's plant anatomy: meristems, cells, and tissues of the plant body: their structure, function, and development. John Wiley & Sons; 2006.
[33] Jung SJ, Kim SH, Chung IM. Comparison of lignin, cellulose, and hemicellulose contents for biofuels utilization among 4 types of lignocellulosic crops. Biomass Bioenergy 2015;83:322–7.
[34] Pfister B, Zeeman SC. Formation of starch in plant cells. Cell Mol Life Sci 2016;73:2781–807.
[35] Farrow TS, Sun C, Snape CE. Impact of CO2 on biomass pyrolysis, nitrogen partitioning, and char combustion in a drop tube furnace. J Anal Appl Pyrolysis 2015;113:323–31.
[36] Deng S, Tan H, Wang X, Yang F, Cao R, Wang Z, et al. Investigation on the fast co-pyrolysis of sewage sludge with biomass and the combustion reactivity of residual char. Bioresour Technol 2017;239:302–10.
[37] Zellagui S, Schönnenbeck C, Zouaoui-Mahzoul N, Leyssens G, Authier O, Thunin E, et al. Pyrolysis of coal and woody biomass under N2 and CO2 atmospheres using a drop tube furnace – experimental study and kinetic modeling. Fuel Process Technol 2016;148:99–109.
[38] Meng H, Wang S, Chen L, Wu Z, Zhao J. Study on product distributions and char morphology during rapid co-pyrolysis of platanus wood and lignite in a drop tube fixed-bed reactor. Bioresour Technol 2016;209:273–81.
[39] Guizani C, Jeguirim M, Valin S, Limousy L, Salvador S. Biomass chars: the effects of pyrolysis conditions on their morphology, structure, chemical properties and reactivity. Energies 2017;10.
[40] Trubetskaya A, Jensen PA, Jensen AD, Garcia Llamas AD, Umeki K, Glarborg P. Effect of fast pyrolysis conditions on biomass solid residues at high temperatures. Fuel Process Technol 2016;143:118–29.
[41] Trubetskaya A, Jensen PA, Jensen AD, Steibel M, Spliethoff H, Glarborg P. Influence of fast pyrolysis conditions on yield and structural transformation of biomass chars. Fuel Process Technol 2015;140:205–14.
[42] Toufiq Reza M, Borrego AG, Wirth B. Optical texture of hydrochar from maize silage and maize silage digestate. Int J Coal Geol 2014;134–135:74–9.
[43] Pohlmann JG, Osório E, Vilela ACF, Diez MA, Borrego AG. Pulverized combustion under conventional (O2/N2) and oxy-fuel (O2/CO2) conditions of biomasses treated at different temperatures. Fuel Process Technol 2017;155:174–82.
[44] Buhre BJP, Hinkley JT, Gupta RP, Nelson PF, Wall TF. Fine ash formation during combustion of pulverised coal-coal property impacts. Fuel 2006;85:185–93.
[45] Jones JM, Pourkashanian M, Rena CD, Williams A. Modelling the relationship of coal structure to char porosity. Fuel 1999;78:1737–44.
[46] Alonso MJG, Borrego AG, Alvarez D, Menéndez R. Pyrolysis behaviour of pulverised coals at different temperatures. Fuel 1999;78:1501–13.
[47] Baltrus JP, Wells AW, Fauth DJ, Diehl JR, White CM. Characterization of carbon concentrates from coal-combustion fly ash. Energy Fuels 2001;15:455–62.
[48] Jenkinson P. A new classification system for biomass and waste materials for their use in combustion. University of Nottingham; 2016.
[49] Ulloa C, Borrego AG, Helle S, Gordon AL, García X. Char characterization and DTF assays as tools to predict burnout of coal blends in power plants. Fuel 2005;84:247–57.
[50] Louw EB, Mitchell GD, Wang J, Winans RE, Mathews JP. Constitution of drop-tube-generated coal chars from vitrinite- and inertinite-rich South African coals. Energy Fuels 2016;30:112–20.
[51] Qian K, Kumar A, Patil K, Bellmer D, Wang D, Yuan W, et al. Effects of biomass feedstocks and gasification conditions on the physiochemical properties of char. Energies 2013;6:3972–86.
[52] Jones JM, Lea-Langton AR, Ma L, Pourkashanian M, Williams A. Combustion of solid biomass: classification of fuels. Pollut. Gener. by Combust. Solid Biomass Fuels. SpringerBriefs Appl. Sci. Technol.. London: Springer-Verlag London; 2014.
[53] Williams O, Newbolt G, Eastwick C, Kingman S, Giddings D, Lormor S, et al. Influence of mill type on densified biomass comminution. Appl Energy 2016;182:219–31.
[54] Holmgren P, Wagner DR, Strandberg A, Molinder R, Wiinikka H, Umeki K, et al. Size, shape, and density changes of biomass particles during rapid devolatilization. Fuel 2017;206:342–51.
[55] Akram M, Tan CK, Garwood R, Thai SM. Vinasse – a potential biofuel – cofiring with coal in a fluidised bed combustor. Fuel 2015;158:1006–15.
[56] Pang CH, Gaddipatti S, Tucker G, Lester E, Wu T. Relationship between thermal behaviour of lignocellulosic components and properties of biomass. Bioresour Technol 2014;172:312–20.
[57] Gomes DI, Detmann E, Valadares Filho S de C, Fukushima RS, de Souza MA, Valente TNP, et al. Evaluation of lignin contents in tropical forages using different analytical methods and their correlations with degradation of insoluble fiber. Anim Feed Sci Technol 2011;168:206–22.
[58] Fukushima RS, Kerley MS. Use of lignin extracted from different plant sources as standards in the spectrophotometric acetyl bromide lignin method. J Agric Food Chem 2011;59:3505–9.
[59] Fang JM, Sun R, Fowler P, Tomkinson J, Hill CAS. Esterification of wheat straw hemicelluloses in the N, N-dimethylformamide/lithium chloride homogeneous system. J Appl Polym Sci 1999;74:2301–11.
[60] Ishizawa CI, Jeoh T, Adney WS, Himmel ME, Johnson DK, Davis MF. Can delignification decrease cellulose digestibility in acid pretreated corn stover? Cellulose 2009;16:677–86.
[61] Lu H, Ip E, Scott J, Foster P, Vickers M, Baxter LL. Effects of particle shape and size on devolatilization of biomass particle. Fuel 2010;89:1156–68.
[62] Perry RH, Green DW. Section 21: Solid-solid operations and processing. Perry Chem. Eng. Handb. 8th ed., McGraw-Hill; 2008, p. 21:47–21:49.
[63] Gera D, Mathur MP, Freeman MC, Robinson A. Effect of large aspect ratio of biomass particles on carbon burnout in a utility boiler. Energy Fuels 2002;16:1523–32.
[64] Yang YB, Sharifi VN, Swithenbank J, Ma LIL, Jones JM, et al. Combustion of a single particle of biomass. Energy Fuels 2008;22:306–16.
[65] Momeni M, Yin C, Kær SK, Hansen TB, Jensen PA, Glarborg P. Experimental study on effects of particle shape and operating conditions on combustion characteristics of single biomass particles. Energy Fuels 2013;27:507–14.
[66] Damstedt B, Pederson JM, Hansen D, Knighton T, Jones J, Christensen C, et al. Biomass cofiring impacts on flame structure and emissions. Proc Combust Inst 2007;31 II:2813–20.
[67] Alvarez D, Borrego AG, Menendez R. Unbiased methods for the morphological description of char structures. Fuel 1997;76:1241–8.
[68] Wu T. Automated char image analysis and the inclusion of char morphology in char burnout modelling. University of Nottingham, 2004.
[69] Jones JM, Bridgeman TG, Darvell LI, Gudka B, Saddawi A, Williams A. Combustion properties of torrefied willow compared with bituminous coals. Fuel Process Technol 2012;101:1–9.
[70] Fisher EM, Dupont C, Darvell LI, Commandré JM, Saddawi A, Jones JM, et al. Combustion and gasification characteristics of chars from raw and torrefied biomass. Bioresour Technol 2012;119:157–65.
[71] Cloke M, Wu T, Barranco R, Lester E. Char characterisation and its application in a coal burnout model. Fuel 2003;82:1989–2000.
[72] Chen WH, Lu KM, Lee WJ, Liu SH, Lin TC. Non-oxidative and oxidative torrefaction characterization and SEM observations of fibrous and ligneous biomass. Appl Energy 2014;114:104–13.
[73] Stach E. Stach's textbook of coal petrology. Berlin: 1982.
[74] Alvarez D, Borrego AG, Mene R, Nacional I, Bailey JG. An unexpected trend in the combustion behavior of hvBb coals as shown by the study of their chars 1998;624:849–55.
[75] Chen H, Wang L. Chapter 3 – Pretreatment Strategies for Biochemical Conversion of Biomass. Technol. Biochem. Convers. Biomass, Elsevier; 2017, p. 21–64.
[76] Cetin E, Gupta R, Moghtaderi B. Effect of pyrolysis pressure and heating rate on radiata pine char structure and apparent gasification reactivity. Fuel 2005;84:1328–34.
[77] Burgess J. Introduction to plant cell development. CUP Archive; 1985.
[78] Schulze ED, Heimann M, Harrison S, Holland E, Lloyd J, Prentice IC, et al. Global biogeochemical cycles in the climate system. Elsevier; 2001.